Magnetization study of nanograined pure and Mn-doped ZnO films: Formation of a ferromagnetic grain-boundary foam

Boris B. Straumal,[1,2,3] Andrei A. Mazilkin,[1,2] Svetlana G. Protasova,[1,2] Ata A. Myatiev,[3] Petr B. Straumal,[3,4] Gisela Schütz,[1] Peter A. van Aken,[1] Eberhard Goering,[1] and Brigitte Baretzky[1]

[1]*Max-Planck-Institut für Metallforschung, Heisenbergstrasse 3, 70569 Stuttgart, Germany*

[2]*Institute of Solid State Physics, Russian Academy of Sciences, Chernogolovka, Moscow District 142432, Russia*

[3]*Moscow Institute of Steel and Alloys, Technological University, Leninsky Prospect 4, 119991 Moscow, Russia*

[4]*Institut für Materialphysik, Universität Münster, Wilhelm-Klemm-Str. 10, D-48149 Münster, Germany*

(Received 17 December 2008; revised manuscript received 7 March 2009; published 14 May 2009)

In order to elucidate room-temperature (RT) ferromagnetism (FM) in ZnO, we have analyzed a multitude of experimental publications with respect to the ratio of grain-boundary (GB) area to grain volume. FM only appears if this ratio exceeds a certain threshold value s_{th}. Based on these important results nanograined pure and Mn-doped ZnO films have been prepared, which reveal reproducible RT FM and magnetization proportional to the film thickness, even for pure ZnO films. Our findings strongly suggest that grain boundaries and related vacancies are the intrinsic origin for RT ferromagnetism.

DOI: 10.1103/PhysRevB.79.205206 PACS number(s): 75.50.Pp, 75.75.+a, 81.05.Je, 81.15.Lm

I. INTRODUCTION

Dietl *et al.*[1] theoretically predicted that ZnO doped by "magnetic" atoms such as Co, Mn, or Fe possess ferromagnetic (FM) behavior with a high Curie temperature T_c above room temperature (RT). This is due to carrier-related FM interactions, where the FM ordering of the transition-metal (TM) ions is induced by a magnetically polarized and by doping a modified ZnO host. Indeed, FM has been experimentally observed in "magnetically" doped ZnO, e.g., with Co,[2] Mn,[3–6] or Fe.[7] Recent theoretical investigations have clarified the importance of O vacancies for magnetic long-range interactions and FM.[8] It was also reported that even doping with "nonmagnetic" atoms such as Cu or Bi leads to RT FM in ZnO.[9–11] FM had also been observed in undoped oxides, especially in HfO_2 (Ref. 12) and more recently even in pure ZnO.[7,13–16] Related calculations confirmed that defects in oxides such as ZnO, TiO_2, HfO_2, and In_2O_3 can lead to FM behavior even without any doping.[17–19] Despite the fact that hundreds of papers devoted to the search of FM in pure and doped ZnO have been published so far, the experimental results are very contradictory and a basic understanding is still missing. Moreover, the well-known problem of TM precipitates in ZnO (see Refs. 20 and 21 and references therein) obscures the situation further. In addition, recent x-ray magnetic circular dichroism (XMCD) investigations have clearly shown that the transition-metal ion in doped ZnO is just paramagnetic and no FM element could be identified.[22] These facts question the original idea of FM order at the TM site induced by conducting electrons. Although oxygen defects are also broadly recognized as a possible reason for the FM behavior of pure and doped ZnO, Tietze *et al.*[22] and Sundaresan *et al.*[23] suggested oxygen defects itself—and not the TM ions—as the intrinsic origin of FM.[12]

II. CRITICAL ANALYSIS OF PUBLISHED DATA: THRESHOLD GRAIN SIZE FOR FERROMAGNETISM IN Mn DOPED AND PURE ZnO

A qualitative literature search reveals that pure and doped ZnO single crystals, or samples obtained by using the conventional powder sintering method (with a particle size of above $\sim 10\ \mu m$), are always diamagnetic or paramagnetic.[24–32] Vice versa, samples obtained by using the pulsed laser deposition (PLD) (Refs. 3–6) exhibit FM in many cases, while ZnO synthesized by wet chemistry methods or chemical vapor deposition (CVD) has intermediate properties; it can be either paramagnetic or FM.[2,33–42]

In order to quantify the defects and grain boundaries (GB) we introduced the specific GB area, s_{GB}, the ratio of grain-boundary area to volume, and determined it from published works devoted to the search of FM in pure and Mn-doped ZnO.[2–69] In the case of single crystals[25,32,38] or doped ZnO films deposited on the ZnO single crystal,[54] no GBs are present, and since formally the s_{GB} value is very large for them, the value $s_{GB}=4\times10^2\ m^2/m^3$ was chosen to indicate data for such single crystals close to the left margin in Fig. 1 (□). The next simplest case are dense (no pores or holes) samples with equiaxial grains (○, ●). The optimal space-filling grain shape for such polycrystals is a polyhedron with 14 faces called tetrakaidecahedron, and the GB area to volume ratio is $s_{GB}=1.65/D$, where D is the mean grain size.[70] By approximation, this formula was applied to dense poreless samples with equiaxial grains as obtained, for example, by sintering (conventional[24,26–28,30,31,36,50,51] or nanopowders[16,37,43]), or for films obtained by pyrolysis.[55] The D values were either directly measured by transmission electron microscopy (TEM) or taken from other referenced published papers [where they could also be determined by TEM or x-ray diffraction (XRD) pattern]. In this case the error bars were shorter than the visible width of the points in Fig. 1. If the polycrystals remain dense, but with elongated[2–7,15,22,38,42,46,53,56–59] or flattened[44,48] grains (△, ▲), the s_{GB} value changes according to the aspect ratio usually quoted in published papers. In case of elongated grains $s_{GB}=1.65a/D$, D is the mean grain width and $a<1$ is the aspect ratio (ratio of grain width to grain height). In the case of flattened grains $s_{GB}=1.65a/D$, $a>1$, (a is the ratio of grain width D to grain height). In a few cases, however, we estimated the aspect ratio by using the micrographs published. If

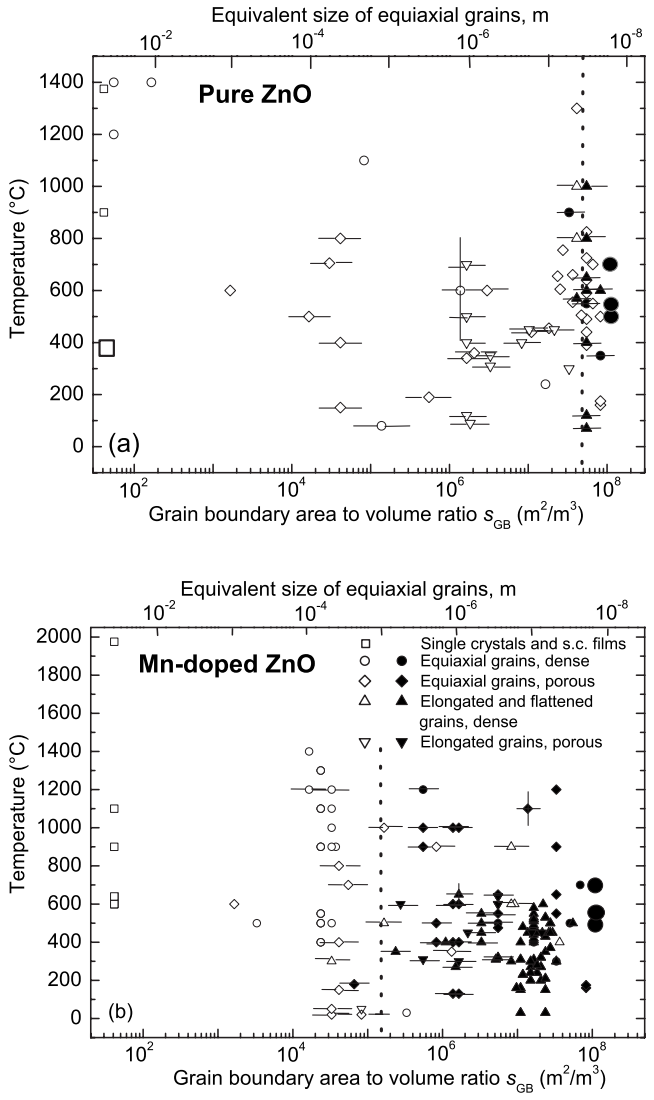

FIG. 1. FM (full symbols) and paramagnetic or diamagnetic (open symbols) behavior of pure and Mn-doped ZnO in dependence on the specific GB area, s_{GB}, the ratio of GB area to volume, at different preparation temperatures T. Vertical lines mark the estimated threshold value s_{th}. Enlarged symbols indicate the experimental data obtained by the investigations of the authors (for symbols and references see text).

the polycrystals consisting of equiaxial grains are porous and not dense, for example, similar to the partly sintered powders (◇, ◆),[33–35,45,49,52,60–64] nanorods, or nanowires (▽, ▼),[13,14,39–41,47,65–68] the s_{GB} value decreases approximately by the porosity coefficient, p, where p varies from 0 for nonsintered powders to 1 for fully compacted polycrystals. p was never quoted in any literature and were estimated using the published micrographs. Indeed, such estimations are rather imprecise and consequently the respective points in Fig. 1 have pronounced error bars.

The results for pure and Mn-doped ZnO are summarized in Fig. 1 in a T-s_{GB} plot (T represents the annealing or synthesis temperature). Indeed, the results clearly reveal a dependence of the FM behavior of pure and Mn-doped ZnO on s_{GB}. The samples are FM only if s_{GB} exceeds a certain threshold value s_{th}. For Mn-doped ZnO, $s_{th}=(2\pm4)\times10^5$ m^2/m^3, while the threshold value for pure ZnO, $s_{th}=(5\pm3)\times10^7$ m^2/m^3, is more than 2 orders of magnitude higher. First indications of a FM behavior in undoped ZnO were published only recently.[2,7,13–16,23] A large area of free surfaces without GBs does not lead to FM, even in extremely small ZnO particles.[24,43] Nonsintered (at least partially) ZnO particles or rods, which do not contain a significant amount of GBs, also do not show significant FM. Similar results were also found for Co-doped ZnO (with $s_{th}=2\times10^6$ m^2/m^3) and will be published elsewhere. Thus, the presence of Mn (or Co) is not necessary for the ferromagnetic properties of ZnO.[22,69] Even pure ZnO can be ferromagnetic, critical is the low grain size (high s_{GB}), and not the doping with magnetic atoms as it was originally supposed. Nevertheless, the presence of Mn or Co in the ZnO lattice facilitates the transition into ferromagnetic state for ZnO and shifts the threshold s_{GB} toward the larger grain size. Thus, for example some authors whose samples had s_{GB} between the values for pure and Mn-doped ZnO observed paramagnetism in pure ZnO and ferromagnetism in Mn-doped ZnO.[41,42] As proposed by Coey *et al.*[17] Mn or Co dopants introduce into ZnO the shallow donor electrons which mediate the ferromagnetic exchange by forming bound magnetic polarons, which overlap to create a spin-split impurity band. However, it follows from Figs. 1(a) and 1(b) that the dopants are not uniformly distributed in ZnO, but mainly segregated in the GBs and thus forming a kind of network inside of the nanograined ZnO. The percolation threshold conditions for the overlapping of polarons will be quite different in such network (or GB foam) in comparison with random distribution of dopants.[17] The evidence of strong Mn and Co segregation in ZnO GBs, especially in nanograined polycrystals, is supported by the observed shift of solubility limit with decreasing grain size.[21,71] Nevertheless, this is highly speculative at the moment but opens new perspectives and solution approaches for puzzling field of ferromagnetism in ZnO.

III. EXPERIMENTAL

In order to prove the results shown in Fig. 1, we prepared our own pure and Mn-doped ZnO samples. Pure ZnO single crystals were grown (at 380 °C) by the hydrothermal method, as well as pure and Mn-doped ZnO thin films consisting of dense equiaxial nanograins, by using the novel method of liquid ceramics.[21] The zinc (II) butanoate diluted in the organic solvent with zinc concentrations between 1 and 4 kg/m^3 was used as a precursor for the preparation of pure ZnO films. For the ZnO films doped with 0.1 and 10 at. % Mn, zinc (II) butanoate solution was mixed with the manganese (III) butanoate solution in respective proportions. The butanoate precursor was deposited onto polycrystalline Al foils and on the (102) sapphire single crystals. The drying at 100 °C in air (about 30 min) was followed by the thermal pyrolysis in the electrical furnace (in air). The pyrolysis was performed at 500 °C, 550 °C, and 600 °C. Similar method was recently proposed for zinc oleates.[72] The Zn and Mn contents in doped oxides were measured by atomic absorption spectroscopy in a Perkin-Elmer spectrom-

eter and electron-probe microanalysis (EPMA). The presence of other magnetic impurities was below 0.001 at. %. During the thorough preparation procedure all possible precautions were taken to exclude any additional FM contaminations (nonmagnetic tweezers, ceramic scissors, etc.). It is known from the literature[2] that the effect of contaminated substrate can completely conceal (hide) the ferromagnetic signal of ZnO itself. We carefully measured the magnetization curves for the blanc substrates and subtracted them from the curves for the ZnO films. The films were greenish and transparent with thicknesses between 50 and 900 nm. The thickness was determined by means of EPMA and edge-on TEM. EPMA investigations were carried out in a Tescan Vega TS5130 MM microscope equipped by the LINK energy-dispersive spectrometer produced by Oxford Instruments. TEM investigations were carried out on a Jeol JEM-4000FX microscope at an accelerating voltage of 400 kV. XRD data were obtained on a Siemens diffractometer (Fe K_α radiation). Evaluation of the grain or particle size (D) from the x-ray peak broadening was performed using the so-called Williamson-Hall approach. In this approach experimental x-ray peak broadening is given as $\beta = 0.9\lambda/D \cos\theta + 4\varepsilon \sin\theta/\cos\theta$ where λ is the x-ray wavelength, θ is the diffraction angle, ε is the lattice strain, and β is the full width at half maximum of the diffraction line.[73]

The magnetic properties were measured on a superconducting quantum interference device (SQUID) (Quantum Design MPMS-7 and MPMS-XL). The magnetic field was applied parallel to the sample plane (in plane). The diamagnetic background signals, generated by the sample holder and the substrate, were carefully subtracted, due to the small absolute magnetic moments measured in the range of 10^{-6}–10^{-4} emu.

IV. RESULTS AND DISCUSSION

Thin nanocrystalline and dense films of pure and Mn-doped ZnO, consisting of equiaxial grains with a mean grain size of about 15 nm, were obtained [see dark field TEM micrograph in Fig. 2(a)]. In addition to the TEM, selected area diffraction [Fig. 2(b)] and XRD were performed on several thin-film samples, which only showed signals from the ZnO wurtzite structure and the respective substrate [see also the radial distribution of the SAED pattern intensity versus scattering vector $k = 2\pi/d$ (Ref. 74) with the positions of diffraction lines for the ZnO wurtzite structure in Fig. 2(c)]. The diffraction rings [Fig. 2(b)] were uniform and no texture and also no other phases could be observed.

The observed FM behavior in pure and doped nanocrystalline as well as dense ZnO films with 0.1 and 10 at. % Mn is depicted in Fig. 3(a). It clearly shows the pronounced FM indicated by the saturation of magnetization (above 1–2 T) and hysteresis behavior (Fig. 4). The saturation magnetization per formula unit (f.u.) was calculated for the ZnO lattice and is about $0.8 \times 10^{-3} \mu_B$/f.u. = 0.06 emu/g for pure ZnO deposited on Al substrate and about $0.9 \times 10^{-3} \mu_B$/f.u. for pure ZnO deposited on the sapphire (102) single crystal. The saturation magnetization is $2 \times 10^{-3} \mu_B$/f.u. = 0.16 emu/g for 0.1 at. % Mn-ZnO and $0.5 \times 10^{-3} \mu_B$/f.u. = 0.04 emu/g for

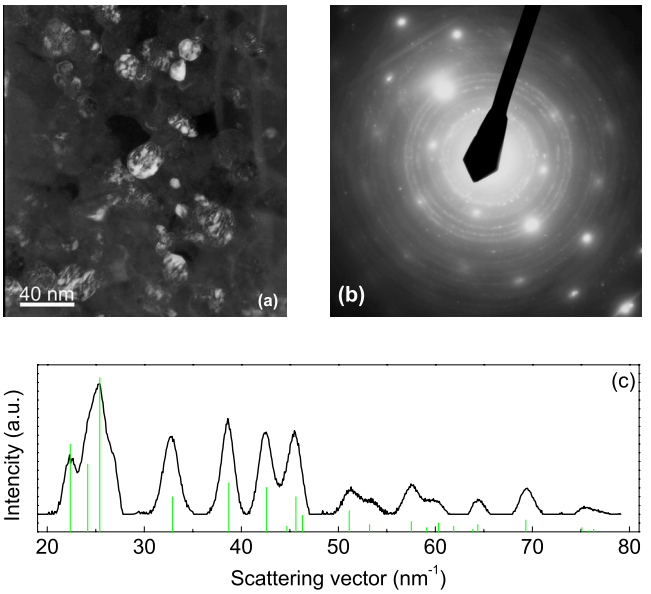

FIG. 2. (Color online) (a) Dark field TEM micrograph of the nanograined pure ZnO thin film deposited on Al foil by using the liquid ceramics method. (b) Selected area electron-diffraction (SAED) pattern and (c) measured radial distribution of the SAED pattern intensity versus scattering vector $k = 2\pi/d$ with the positions of diffraction lines for the ZnO wurtzite structure (vertical lines). No texture is visible, only the rings for the ZnO wurtzite structure are present. Light spots originated from the Al substrate.

10 at. % Mn-ZnO with a grain size of 15 nm. These results are in agreement with the values obtained by other methods for Mn-doped samples.[4,5,34,46,48,51] In Fig. 3(b) the original magnetization curve for pure ZnO [black squares, both in Figs. 3(a) and 3(b)] is shown together with the magnetization curve for the bare Al substrate (after subtraction of diamagnetic contribution). The data in Fig. 3(b) are given in emu/cm^2 in order to facilitate the comparison with contribution of ferromagnetic impurities in the substrate and with the data of other papers where the magnetization per volume or area of samples is given. The observed saturation magnetization for pure ZnO is about 0.3 emu/cm^3 or 0.05 emu/g, which is close to the values observed for pure ZnO obtained by electrodepisition+oxidation (1 emu/cm^3),[13] PLD (1 emu/cm^3),[15] and higher than the values for pure ZnO obtained by the hydrothermal method (0.004 emu/g),[14] the aqueous carboxylate gelation route with subsequent firing at 550 °C (0.0015 emu/g) (Ref. 29) or the surfactant-free wet chemical method (0.0015 emu/g).[16]

Saturation magnetization increases linearly with the thickness (i.e., mass) of the ZnO film as depicted in the inset of Fig. 3. Magnetization curves for pure ZnO films demonstrate hysteresis with coercive fields H_c of about 0.02 T for the ZnO film on sapphire substrate [Fig. 4(a)] and H_c of about 0.01 T for the ZnO film on Al substrate [Fig. 4(b)]. Only the enlarged central part of magnetization curves is given in Fig. 4 in order to clearly show the coercivity values. These values are similar or higher than the coercivity obtained by other authors for pure ZnO (H_c=0.02 T,[16,29] H_c=0.01 T,[15] H_c =0.005 T).[13,14] It can be due to the smaller grain size and higher s_{GB} in our films [see Fig. 1(a)]. Below room tempera-

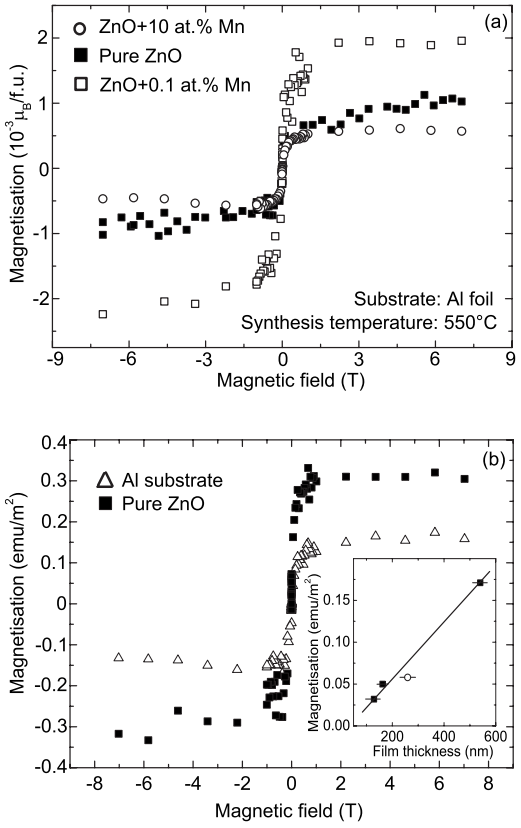

FIG. 3. (a) Magnetization (calibrated in $10^{-3}\mu_B$/f.u.) at room temperature for pure ZnO thin film as well as for ZnO thin films doped with 0.1 and 10 at. % Mn. The curves were obtained after subtracting the magnetic contribution from the substrate and the sample holder. The saturation magnetization is $2\times10^{-3}\mu_B$/f.u. =0.16 emu/g for 0.1 at. % Mn-ZnO, $0.5\times10^{-3}\mu_B$/f.u. =0.04 emu/g for 10 at. % Mn-ZnO, and $0.8\times10^{-3}\mu_B$/f.u. =0.06 emu/g for pure ZnO deposited on Al substrate. (b) Magnetization per area (calibrated in emu/m^2) at room temperature for pure ZnO thin film [black squares, both in Figs. 3(a) and 3(b)] and for the bare Al substrate (after subtraction of diamagnetic contribution). Inset: dependence of the RT magnetization per area unit (calibrated in emu/m^2, after subtracting the magnetic contribution from the substrate and the sample holder) on the film thickness (squares—pure ZnO; circle—ZnO doped by 10 at. % Mn).

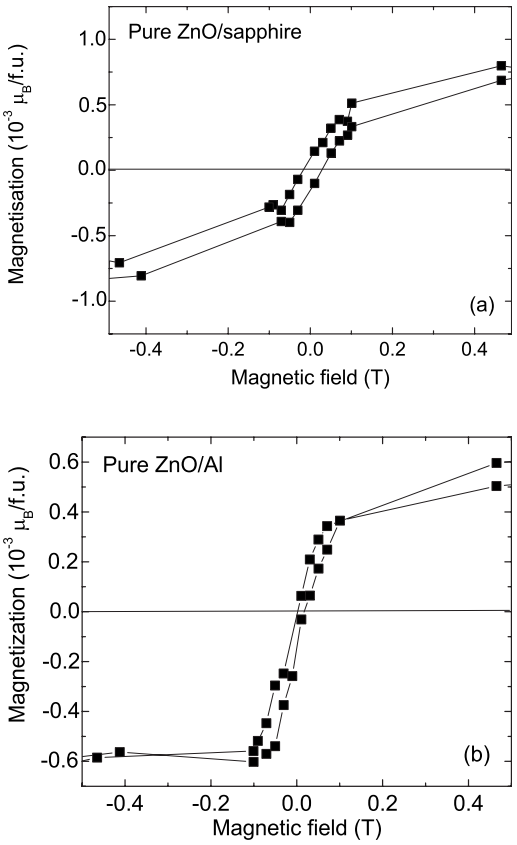

FIG. 4. (a) RT magnetic hysteresis for pure ZnO deposited on the sapphire single crystal. (b) RT magnetic hysteresis for pure ZnO deposited on the aluminum foil. Only the enlarged central part of magnetization curves is given in order to clearly show the coercivity values.

ture (40 K), the saturation magnetization of the pure ZnO film deposited on the sapphire substrate increases by about 40%, suggesting a Curie temperature T_c far above room temperature. The produced nanograined dense ZnO films possess a very reproducible FM behavior with high T_c and a high coercive field which is hardly sensitive to the synthesis temperature, type of substrate or film thickness.

The results on the magnetic properties of pure and Mn-doped ZnO samples marked by large symbols were added to Fig. 1. As expected, the pure ZnO single crystals show pure diamagnetic behavior without any evidence of FM. The corresponding point (large open square) was drawn in the left part of Fig. 1 using the value of $s_{GB}=4\times10^2$ m^2/m^3. This value was formally assigned to the single crystals since they do not contain any GBs in order to indicate data for such samples close to the left margin in Fig. 1 (□).

The results obtained for pure and Mn-doped films were also added into Fig. 1. Due to the extremely small mean grain sizes of 15 nm, the calculated corresponding value for the GB area to volume ratio is rather high, $s_{GB}=1.1\times10^8$ m^2/m^3, and exceeds the respective s_{th} values for pure as well as for Mn-doped ZnO. Consequently, all thin-film samples of pure and Mn-doped ZnO clearly reveal FM behavior at RT and are therefore marked as full circles.

In previously published literature the FM magnetization was usually scaled to the amount of transition-metal ions within the sample, which typically lies in the range of $0.1-1\mu_B$/TM ion. Typical TM dopant concentrations without precipitations usually lie in the 5%–10% region. However, this normalization is highly questionable because recently and carefully performed XMCD experiments on highly FM samples indicate that the TM ions do not provide any significant element specific FM moment.[22] In order to roughly compare our results with those reported elsewhere, we scaled the FM moments of $0.1-1\mu_B$/TM ion cited in the literature to the number of formula units. By assuming a typical concentration value of 5% TM, a 20 times smaller magnetization per formula unit is obtained, which is of the same order of magnitude as the FM moments presented in the current investigation. Therefore, we can conclude that the FM moment of the samples reported in the literature is com-

parable to the GB area related values estimated in the current work. Our results, i.e., FM in pure ZnO and a threshold value for the specific GB area, strongly support the idea that FM originates through crystallographic imperfections, and the moments are located at vacancies present in GBs.

Furthermore, we can conclude that the crystalline ZnO grains are nonmagnetic and surrounded by a FM foamlike GB network. Following this idea, we can roughly estimate the amount of GBs necessary to form such a magnetic foam. Assuming a GB thickness of 0.5 nm and grain sizes of about 50 nm, the volume content of these GBs is about 5%–10%.[44] If we estimate about two excess electrons for every missing oxygen atom[8]), up to $2\mu_B$ per vacancy can be expected, ensuring in principle the necessary magnetic moment to explain the experimental results. Nevertheless, further theoretical and experimental investigations are required to prove this concept of a magnetic foam.

ACKNOWLEDGMENTS

The authors would like to thank the Russian Foundation for Basic Research (Contracts No. 08-08-90105 and No. 08-08-91302) and the Deutsche akademische Austauschdienst (DAAD) for their financial support to these investigations and relating travel. The authors also cordially thank S. Z. Shmurak, D. Goll, A. Nekrasov, Th. Dragon, A. Breitling, M. Kelsch, J. Breithaupt, and U. Salzberger.

[1] T. Dietl, H. Ohno, F. Matsukura, J. Cibert *et al.*, Science **287**, 1019 (2000).
[2] Y. Belghazi, G. Schmerber, S. Colis, J. L. Rehspringer *et al.*, Appl. Phys. Lett. **89**, 122504 (2006).
[3] H. Schmidt, M. Diaconu, H. Hochmuth, M. Lorenz, A. Setzer, P. Esquinazi, A. Pöppl, D. Spemann, K.-W. Nielsen, R. Gross, G. Wagner and M. Grundmann, Superlattices Microstruct. **39**, 334 (2006).
[4] A. K. Pradhan, D. Hunter, K. Zhang, J. B. Dadson *et al.*, Appl. Surf. Sci. **252**, 1628 (2005).
[5] M. Diaconu, H. Schmidt, H. Hochmuth, M. Lorenz *et al.*, J. Magn. Magn. Mater. **307**, 212 (2006).
[6] M. Diaconu, H. Schmidt, H. Hochmuth, M. Lorenz *et al.*, Thin Solid Films **486**, 117 (2005).
[7] N. H. Hong, J. Sakai, and V. Brizé, J. Phys.: Condens. Matter **19**, 036219 (2007).
[8] C. D. Pemmaraju, R. Hanafin, T. Archer, H. B. Braun, and S. Sanvito, Phys. Rev. B **78**, 054428 (2008).
[9] C. Xu, J. Chun, D. Kim, B. Chon *et al.*, Appl. Phys. Lett. **91**, 153104 (2007).
[10] D. L. Hou, X. J. Ye, X. Y. Zhao, H. J. Meng *et al.*, J. Appl. Phys. **102**, 033905 (2007).
[11] T. S. Herng, S. P. Lau, S. F. Yu, J. S. Chen *et al.*, J. Magn. Magn. Mater. **315**, 107 (2007).
[12] M. Venkatesan, C. B. Fitzgerald, and J. M. D. Coey, Nature (London) **430**, 630 (2004).
[13] J. B. Yi, H. Pan, J. Y. Lin, J. Ding *et al.*, Adv. Mater. **20**, 1170 (2008).
[14] Z. Yan, Y. Ma, D. Wang, J. Wang *et al.*, Appl. Phys. Lett. **92**, 081911 (2008).
[15] Q. Y. Xu, H. Schmidt, S. Q. Zhou, K. Potzger *et al.*, Appl. Phys. Lett. **92**, 082508 (2008).
[16] Z. J. Yan, Y. W. Ma, D. L. Wang, J. Wang *et al.*, J. Phys. Chem. C **112**, 9219 (2008).
[17] J. M. D. Coey, M. Venkatesan, and C. B. Fitzgerald, Nat. Mater. **4**, 173 (2005).
[18] R. Monnier and B. Delley, Phys. Rev. Lett. **87**, 157204 (2001).
[19] I. S. Elfimov, S. Yunoki, and G. A. Sawatzky, Phys. Rev. Lett. **89**, 216403 (2002).
[20] M. Ivill, S. J. Pearton, S. Rawal, L. Leu *et al.*, New J. Phys. **10**, 065002 (2008).
[21] B. B. Straumal, A. A. Mazilkin, S. G. Protasova, A. A. Myatiev *et al.*, Acta Mater. **56**, 6246 (2008).
[22] T. Tietze, M. Gacic, G. Schütz, G. Jakob *et al.*, New J. Phys. **10**, 055009 (2008).
[23] A. Sundaresan, R. Bhargavi, N. Rangarajan, U. Siddesh, and C. N. R. Rao, Phys. Rev. B **74**, 161306(R) (2006).
[24] J. Alaria, P. Turek, M. Bernard, M. Bouloudenine *et al.*, Chem. Phys. Lett. **415**, 337 (2005).
[25] M. H. Kane, W. E. Fenwick, M. Strassburg, B. Nemeth, R. Varatharajan, Q. Song, D. J. Keeble, H. El-Mkami, M. G. Smith, Z. J. Zhang, J. Nause, C. J. Summers and I. T. Ferguson, Phys. Status Solidi B **244**, 1462 (2007).
[26] S. C. Wi, J. S. Kang, J. H. Kim, S. S. Lee *et al.*, Phys. Status Solidi B **241**, 1529 (2004).
[27] Y. B. Zhang, T. Sritharan, and S. Li, Phys. Rev. B **73**, 172404 (2006).
[28] S. Kolesnik and B. Dabrowski, J. Appl. Phys. **96**, 5379 (2004).
[29] D. Sanyal, M. Chakrabarti, T. K. Roy, and A. Chakrabarti, Phys. Lett. A **371**, 482 (2007).
[30] J. H. Yang, L. Y. Zhao, Y. J. Zhang, and Y. X. Wang, Solid State Commun. **143**, 566 (2007).
[31] S. Riyadi, M. Muafif, A. A. Nugroho, and A. Rusydi, J. Phys.: Condens. Matter **19**, 476214 (2007).
[32] T. Tamura and H. Ozaki, J. Phys.: Condens. Matter **21**, 026009 (2009).
[33] M. Peiteado, A. C. Caballero, and D. Makovec, J. Eur. Ceram. Soc. **27**, 3915 (2007).
[34] K. C. Barick and D. Bahadur, J. Nanosci. Nanotechnol. **7**, 1935 (2007).
[35] K. P. Bhatti, S. Chaudhary, D. K. Pandya, and S. C. Kashyap, Solid State Commun. **140**, 23 (2006).
[36] J. L. Costa-Kramer, F. Briones, J. F. Fernandez, A. C. Caballero *et al.*, Nanotechnology **16**, 214 (2005).
[37] M. Pal and M. Pal, Jpn. J. Appl. Phys., Part 1 **44**, 7901 (2005).
[38] A. I. Savchuk, P. N. Gorley, V. V. Khomyak, K. S. Ulyanytsky *et al.*, Mater. Sci. Eng., B **109**, 196 (2004).
[39] Y. J. Kang, D. S. Kim, S. H. Lee, J. Park *et al.*, J. Phys. Chem. C **111**, 14956 (2007).
[40] G. Clavel, N. Pinna, and D. Zitoun, Phys. Status Solidi A **204**, 118 (2007).
[41] D. F. Wang, S. Y. Park, H. W. Lee, Y. S. Lee, V. D. Lam and Y.

P. Lee, Phys. Status Solidi A **204**, 4029 (2007).
[42] N. Gopalakrishnan, J. Elanchezhiyan, K. P. Bhuvana, and T. Balasubramanian, Scr. Mater. **58**, 930 (2008).
[43] G. Lawes, A. S. Risbud, A. P. Ramirez, and R. Seshadri, Phys. Rev. B **71**, 045201 (2005).
[44] S. Venkataraj, N. Ohashi, I. Sakaguchi, Y. Adachi *et al.*, J. Appl. Phys. **102**, 014905 (2007).
[45] G. Glaspell, P. Dutta, and A. Manivannan, J. Cluster Sci. **16**, 523 (2005).
[46] K. Masuko, A. Ashida, T. Yoshimura, and N. Fujimura, J. Magn. Magn. Mater. **310**, E711 (2007).
[47] C. J. Cong and K. L. Zhang, Phys. Status Solidi B **243**, 2764 (2006).
[48] A. Che Mofor, A. El-Shaer, A. Bakin, H.-H. Wehmann, H. Ahlers, U. Siegner, S. Sievers, M. Albrecht, W. Schoch, N. Izyumskaya, V. Avrutin, J. Stoemenos and A. Waag, Superlattices Microstruct. **39**, 381 (2006).
[49] D. D. Sarma, R. Viswanatha, S. Sapra, A. Prakash *et al.*, J. Nanosci. Nanotechnol. **5**, 1503 (2005).
[50] D. P. Joseph, G. S. Kumar, and C. Venkateswaran, Mater. Lett. **59**, 2720 (2005).
[51] S. W. Yoon, S.-B. Cho, S. C. We, S. Yoon *et al.*, J. Appl. Phys. **93**, 7879 (2003).
[52] O. D. Jayakumar, H. G. Salunke, R. M. Kadam, M. Mohapatra *et al.*, Nanotechnology **17**, 1278 (2006).
[53] S. Thota, T. Dutta, and J. Kumar, J. Phys.: Condens. Matter **18**, 2473 (2006).
[54] K. Masuko, A. Ashida, T. Yoshimura, and N. Fujimura, J. Appl. Phys. **103**, 043714 (2008).
[55] P. Thakur, K. H. Chae, M. Subramanian, R. Jayavel *et al.*, J. Korean Phys. Soc. **53**, 2821 (2008).
[56] S. Y. Park, H. W. Lee, and J. Y. Rhee, J. Korean Phys. Soc. **51**, 1497 (2007).
[57] J. Elanchezhiyan, K. P. Bhuvana, N. Gopalakrishnan, and T. Balasubramanian, Mater. Lett. **62**, 3379 (2008).
[58] G. H. Ji, Z. B. Gu, M. H. Lu, D. Wu *et al.*, J. Phys.: Condens. Matter **20**, 425207 (2008).
[59] J. C. Pivin, G. Socol, I. Mihailescu, P. Berthet *et al.*, Thin Solid Films **517**, 916 (2008).
[60] M. D. Mukadam and S. M. Yusuf, Physica B **403**, 2602 (2008).
[61] Y. Zhang, E. W. Shi, and Z. Z. Chen, J. Cryst. Growth **310**, 2928 (2008).
[62] L. B. Duan, G. H. Rao, J. Yu, and Y. C. Wang, J. Appl. Phys. **102**, 103907 (2007).
[63] B. Babic-Stojic, D. Milivojevic, J. Blanusa, and V. Spasojevic, J. Phys.: Condens. Matter **20**, 235217 (2008).
[64] E. Schlenker, A. Bakin, H. Schmid, and W. Mader, Appl. Phys. A: Mater. Sci. Process. **91**, 375 (2008).
[65] D. F. Wang, S. Y. Park, and Y. P. Lee, J. Korean Phys. Soc. **53**, 2257 (2008).
[66] H. L. Yan, J. B. Wang, X. L. Zhong, and Y. C. Zhou, Appl. Phys. Lett. **93**, 142502 (2008).
[67] Y. J. Kang, D. S. Kim, S. H. Lee, and J. Park, J. Phys. Chem. C **111**, 14956 (2007).
[68] I. Djerdj, G. Garnweitner, D. Arcon, and M. Pregelj, J. Mater. Chem. **18**, 5208 (2008).
[69] G. Mayer, M. Fonin, S. Foss, U. Rüdiger, and E. Goering, IEEE Trans. Magn. **44**, 2700 (2008).
[70] W. F. Hosford, *Materials Science: An Intermediate Text* (Cambridge University Press, Cambridge, England, 2007), p. 15.
[71] B. B. Straumal, B. Baretzky, A. A. Mazilkin, S. G. Protasova, A. A. Myatiev, and P. B. Straumal, J. Eur. Ceram. Soc. **29**, 1963 (2009).
[72] W. S. Chiu, P. S. Khiew, D. Isa, M. Cloke *et al.*, Chem. Eng. J. **142**, 337 (2008).
[73] A. Soyer, J. Appl. Crystallogr. **28**, 244 (1995).
[74] J. L. Lábár, Microsc. Microanal. **14**, 287 (2008).